Structural Engineering and Mechanics, *Vol. 52, No. 3 (2014) 573-593*
DOI: http://dx.doi.org/10.12989/sem.2014.52.3.573

Pounding between adjacent buildings of varying height coupled through soil

Sadegh Naserkhaki*[1,2], Marwan El-Rich[1], Farah N.A. Abdul Aziz[2] and Hassan Pourmohammad[3]

[1]*Department of Civil and Environmental Engineering, Faculty of Engineering, University of Alberta, Edmonton, Canada*
[2]*Department of Civil Engineering, Faculty of Engineering, Universiti Putra Malaysia, Serdang, Malaysia*
[3]*Department of Civil Engineering, Faculty of Engineering, Islamic Azad University, Karaj Branch, Karaj, Iran*

(Received February 20, 2013, Revised June 13, 2014, Accepted July 20, 2014)

Abstract. Pounding between adjacent buildings is a significant challenge in metropolitan areas because buildings of different heights collide during earthquake excitations due to varying dynamic properties and narrow separation gaps. The seismic responses of adjacent buildings of varying height, coupled through soil subjected to earthquake-induced pounding, are evaluated in this paper. The lumped mass model is used to simulate the buildings and soil, while the linear visco-elastic contact force model is used to simulate pounding forces. The results indicate while the taller building is almost unaffected when the shorter building is very short, it suffers more from pounding with increasing height of the shorter building. The shorter building suffers more from the pounding with decreasing height and when its height differs substantially from that of the taller building. The minimum required separation gap to prevent pounding is increased with increasing height of the shorter building until the buildings become almost in-phase. Considering the soil effect; pounding forces are reduced, displacements and story shears are increased after pounding, and also, minimum separation gap required to prevent pounding is increased.

Keywords: pounding; adjacent buildings; tall building; short building; separation gap; seismic response; Fixed-Based (FB); Structure-Soil-Structure Interaction (SSSI)

1. Introduction

Pounding is the collision of adjacent buildings when they vibrate out-of-phase and the separation gap between them is less than the minimum distance required for them to vibrate freely due to earthquake excitation; this phenomenon has caused damage to buildings during almost every earthquake. Not only was pounding damage to adjacent buildings reported during past earthquakes (Kasai and Maison 1997, Rosenblueth and Meli 1986), but evidence of such pounding has also been directly observed in recent earthquakes around the world (Cole *et al.* 2012, Mix *et al.* 2011, Celebi *et al.* 2010, Zhao *et al.* 2009). The majority of these pounding occurrences refer to pounding between adjacent buildings of different heights, which is called taller adjacent building pounding. Pounding between adjacent buildings of different heights is of concern in metropolitan

*Corresponding author, Ph.D. Student, E-mail: s.naserkhaki@ualberta.ca

http://www.techno-press.org/?journal=sem&subpage=8 ISSN: 1225-4568 (Print), 1598-6217 (Online)

areas where buildings are densely located and new tall buildings are rising adjacent to existing short buildings.

Jeng and Tzeng (2000) have estimated that the highest proportion of pounding occurrences in Taipei (60%) belonged to adjacent buildings with substantially different heights. Moreover, Mirtaheri *et al.* (2012) have predicted that pounding between adjacent buildings of different heights is a significant issue in buildings on Karimkhan Avenue in Tehran during strong earthquakes. The evaluation of seismic responses in adjacent buildings of varying heights due to pounding, and the implementation of relevant safety measures, is an important issue to resolve in metropolitan areas.

Height differences in adjacent buildings (i.e., different dynamic properties) lead to out-of-phase seismic responses and, consequently, pounding between the buildings if the separation gap is narrow. Both the probability and intensity of the pounding depend on the building height difference. When the height difference between buildings is only one or two stories, the buildings vibrate almost in-phase and the probability and intensity of the pounding is low. On the other hand, there is a high probability and intensity of pounding if the difference in height between adjacent buildings is more than two stories and they vibrate out-of-phase. Therefore, variation in the heights of adjacent buildings is a major parameter to be considered in the pounding problem between adjacent buildings. This issue becomes more critical if the soil beneath adjacent buildings is relatively soft because the soil alters the phase difference in the buildings' seismic responses (Naserkhaki *et al.* 2012a, Jeng and Kasai 1996) and causes larger building displacements (Naserkhaki *et al.* 2012a, Savin 2003), which increase the likelihood of pounding.

Many researchers have explored the adjacent building pounding issue and studied its aspects numerically previously. Maison and Kasai (1990) conducted one of the primary studies on this problem. They evaluated the seismic responses of a University of California Medical Center building that had experienced pounding with an adjacent rigid building. The building was connected to the top floor of the adjacent rigid building by a contact force model and was simulated with a linear mass, damping and spring system. Maison and Kasai extended their work by considering flexible behavior for both buildings in 1992. Pounding was found to amplify drifts, story shears and overturning moments in the stories above the potential pounding location, and these effects were deemed critical factors that must be taken into consideration to ensure the safe design of a building.

Among the numerous existing works on the adjacent building pounding issue, studies by Naserkhaki *et al.* (2013a, b) , Polycarpou and Komodromos (2010), Favvata *et al.* (2009), Abdel Raheem (2006), Karayannis and Favvata (2005a, b), Mouzakis and Papadrakakis (2004), Filiatrault *et al.* (1995), Anagnostopoulos and Spiliopoulos (1992) refer to the evaluation of seismic responses in adjacent buildings with different heights. Changes in the story height have been considered by Favvata *et al.* (2009), Karayannis and Favvata (2005b) where they investigated inter-story height pounding between two adjacent RC buildings. Except these height changes, each study used a unique configuration of adjacent buildings to investigate their seismic responses due to pounding, but height variations in these adjacent buildings (i.e. variation in building stories) were not concern of these works.

Karayannis and Favvata (2005b) initiated the discussion on pounding of RC buildings with varying height. From the parametric study reported in this work it was deduced that no safe conclusions could be extracted about the influence of small changes of the number of stories of the tall building on the demands for ductility and shear strength of the columns that suffered the hit. High increase of the number of stories of the tall building (from 6 to 12 stories) in all the examined

pounding cases had decreased substantially the demands for ductility and shear strength of the suffered columns, up to the point that the pounding did not really affect these demands. Study by Naserkhaki *et al.* (2012b) confirms this conclusion in another way specially when one building is significantly taller than the shorter one. They state when the difference in building height is significant, the taller building is less affected whereas the shorter building is more affected from the pounding. These conclusions have been reported for the buildings with fixed based without considerations of soil flexibility.

Naserkhaki *et al.* (2012a), Shakya and Wijeyewickrema (2009), Rahman *et al.* (2001) highlight soil effects on the seismic responses of adjacent buildings coupled through the soil and subjected to pounding. The main concern of these researchers was the soil effects on building pounding rather than height variations in adjacent buildings in different configurations. In conclusion, the seismic responses of adjacent buildings with varying heights coupled through the soil subjected to earthquake-induced pounding, though a significant problem in large cities, are still unclear and demand further study.

The aim of this research is to evaluate the seismic responses of adjacent buildings of varying heights subjected to earthquake-induced pounding. The adjacent buildings are assumed to be constructed on either rock/hard soil (i.e., adjacent buildings are fixed-based, FB) or soft soil (i.e., adjacent buildings are coupled through the soil with structure-soil-structure interaction, SSSI). An analytical model of adjacent buildings coupled through the soil is developed. Finally, different configurations of adjacent buildings with varying heights are analyzed, effect of pounding on the building responses is discussed and the minimum required separation gap to prevent pounding and differences in the seismic responses of adjacent buildings of varying heights subjected to pounding are clarified.

2. Formulation and solution

2.1 Equation of motion of two adjacent buildings coupled through the soil during earthquake induced pounding

The adjacent buildings and the soil are modeled as shear buildings and discrete soil, respectively, with the concentrated mass, dashpot and linear spring (Fig. 1). The connection between each building and the soil occurs through interaction forces of equal magnitude but opposite directions in the building and the soil. These interaction forces arise from inertial forces corresponding to the masses of the building and the soil, called inertial interaction (Naserkhaki and Pourmohammad 2012, Clough and Penzien 2003). Moreover, the adjacent buildings are coupled through the soil and response of each building affects the other, a setup that is called structure-soil-structure interaction or SSSI effect (Naserkhaki and Pourmohammad 2012, Padron *et al.* 2009). The pounding force at each floor level is simulated by a linear visco-elastic contact force model (Fig. 1). With these assumptions, equation of motion of two adjacent buildings coupled through the soil during earthquake induced pounding is given by

$$\boldsymbol{M_{bsb}\ddot{U}_{bsb} + C_{bsb}\dot{U}_{bsb} + K_{bsb}U_{bsb} + F = -(M_{bsb}v_{bsb} + v_{fbsb})\ddot{u}_g(t)} \quad (1)$$

$\boldsymbol{F}$ is the vector of pounding forces which is developed when the adjacent buildings pound together. $\boldsymbol{M_{bsb}}$, $\boldsymbol{C_{bsb}}$, and $\boldsymbol{K_{bsb}}$ are the mass, damping and stiffness matrices of the adjacent buildings, respectively. $\boldsymbol{\ddot{U}_{bsb}}$, $\boldsymbol{\dot{U}_{bsb}}$ and $\boldsymbol{U_{bsb}}$ are the acceleration, velocity and displacement vectors of the

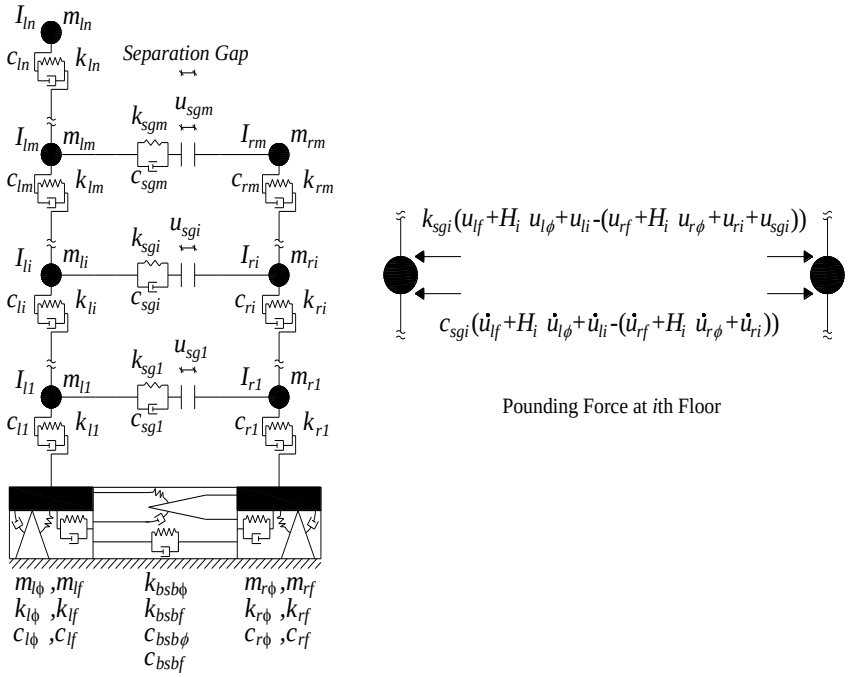

Fig. 1 Analytical model of the adjacent buildings coupled through the soil

adjacent buildings, respectively. $\boldsymbol{v_{bsb}}$ and $\boldsymbol{v_{fbsb}}$ are the influence vectors of the buildings and soil, respectively and $\ddot{\boldsymbol{u}}_{\boldsymbol{g}}(\boldsymbol{t})$ is the earthquake acceleration.

As shown in Fig. 1, pounding force that acts at the pounding instant is equal for pounded adjacent floors but in opposite direction. This pounding force is simulated by a linear visco-elastic contact force model that consists of a linear spring to account for pounding induced elastic force and a dashpot to represent energy dissipation during the pounding. It is activated only if the separation gap is closed and two adjacent buildings collide together, developing pounding forces. Simulating the pounding force while also considering energy dissipation during the pounding and its efficiency and practicality are advantages of the linear visco-elastic contact force model. Its only deficiency is in providing tension forces at the end of the pounding that have no physical meaning, which can be ignored (Komodromos *et al.* 2007). The relationship between the pounding force and displacement of the contact force model is shown in Fig. 2. The pounding force that is developed immediately after pounding is correlated to the relative displacements (i.e., elastic force) and relative velocities (i.e., energy dissipation) between the adjacent buildings as

$$\boldsymbol{F} = \boldsymbol{C_p}\dot{\boldsymbol{U}}_{\boldsymbol{bsb}} + \boldsymbol{K_p}(\boldsymbol{U_{bsb}} - \boldsymbol{U_{sg}}) \tag{2}$$

$\boldsymbol{C_p}$ and $\boldsymbol{K_p}$ are the damping and stiffness matrices of the pounding forces, respectively, and $\boldsymbol{U_{sg}}$ is the vector of separation gap. Finally, substituting the vector of pounding forces ($\boldsymbol{F}$) into the Eq. (1) gives

$$\begin{aligned}\boldsymbol{M_{bsb}}\ddot{\boldsymbol{U}}_{\boldsymbol{bsb}} + (\boldsymbol{C_{bsb}} + \boldsymbol{C_p})\dot{\boldsymbol{U}}_{\boldsymbol{bsb}} + (\boldsymbol{K_{bsb}} + \boldsymbol{K_p})\boldsymbol{U_{bsb}} \\ = -(\boldsymbol{M_{bsb}}\boldsymbol{v_{bsb}} + \boldsymbol{v_{fbsb}})\ddot{\boldsymbol{u}}_{\boldsymbol{g}}(\boldsymbol{t}) + \boldsymbol{K_p}\boldsymbol{U_{sg}}\end{aligned} \tag{3}$$

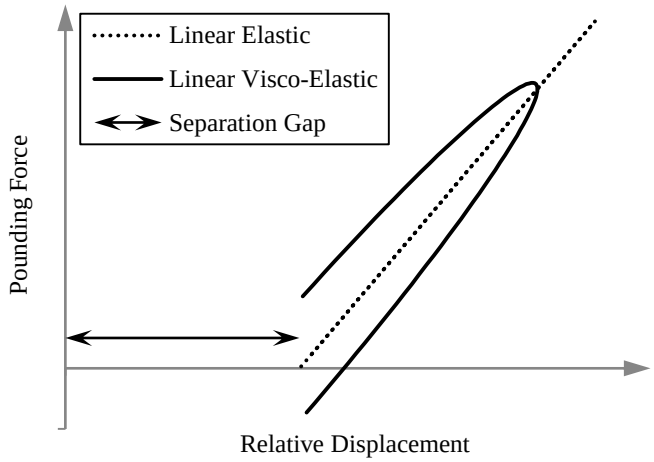

Fig. 2 Relationship between pounding force and displacement (Naserkhaki *et al.* 2012b)

This equation is final representation of the equation of motion of two adjacent buildings coupled through the soil during earthquake-induced pounding. The terms and parameters of this equation are determined in the following.

The damping matrix of the pounding forces ($\boldsymbol{C_p}$) is

$$\boldsymbol{C_p} = \begin{bmatrix} \boldsymbol{c_{p1}} & \boldsymbol{c_{p12}} & \mathbf{0} & -\boldsymbol{c_{p1}} & -\boldsymbol{c_{p12}} \\ & \boldsymbol{c_{p2}} & \mathbf{0} & -\boldsymbol{c_{p21}} & -\boldsymbol{c_{p2}} \\ & & \mathbf{0} & \mathbf{0} & \mathbf{0} \\ & \boldsymbol{SYM.} & & \boldsymbol{c_{p1}} & \boldsymbol{c_{p12}} \\ & & & & \boldsymbol{c_{p2}} \end{bmatrix} \tag{4}$$

where

$$\boldsymbol{c_{p1}} = \begin{bmatrix} \sum_{i=1}^{m} H_i^2 c_{sgi} & \sum_{i=1}^{m} H_i \ c_{sgi} \\ \sum_{i=1}^{m} H_i \ c_{sgi} & \sum_{i=1}^{m} c_{sgi} \end{bmatrix} \tag{5}$$

$$\boldsymbol{c_{p2}} = \begin{bmatrix} c_{sg1} & \cdots & 0 \\ \vdots & \ddots & \vdots \\ 0 & \cdots & c_{sgm} \end{bmatrix} \tag{6}$$

$$\boldsymbol{c_{p12}} = \boldsymbol{c_{p21}^T} = \begin{bmatrix} H_1 c_{sg1} & \cdots & H_m c_{sgm} \\ c_{sg1} & \cdots & c_{sgm} \end{bmatrix} \tag{7}$$

H_i is the height of *i*th floor from the center of gravity of the soil. c_{sgi} is the damping coefficient of the pounding force which can be determined from the mass and stiffness of the adjacent buildings at the *i*th floor and the coefficient of restitution (Anagnostopoulos 1988)

$$c_{sgi} = 2\xi \sqrt{k_{sgi} \frac{m_{li} m_{ri}}{m_{li} + m_{ri}}} \tag{8}$$

where

$$\xi = -\frac{\ln(e)}{\sqrt{\pi^2 + \ln(e^2)}} \tag{9}$$

m_{li} and m_{ri} are the mass of ith floor of the left and right buildings, respectively. k_{sgi} is the contact stiffness of the contact force model. The contact stiffness is a term without a special calculation procedure. It has been suggested to be proportional to either the axial stiffness of the pounded diaphragm (Muthukumar and DesRoches 2006, Ruangrassamee and Kawashima 2003, Zhu *et al*. 2002, Maison and Kasai 1992, Maison and Kasai 1990) or the lateral stiffness of the pounded floor (Naserkhaki *et al*. 2012b, Anagnostopoulos 1988). A contact stiffness of 10000 MN/m is chosen for this study which is almost 55 times the lateral stiffness of the buildings at each story (Naserkhaki *et al*. 2012b). e is the coefficient of restitution that is the ratio of the contact and separation velocities (i.e., the starting and ending velocities) of the pounding. The coefficient of restitution ranges between 1 for pure elastic and 0 for pure plastic poundings. Its values in practical applications can fall between 0.5 and 1.0 (DesRoches and Muthukumar 2002, Rajalingham and Rakheja 2000, Nguyen *et al*. 1986, Anagnostopoulos and Spiliopoulos 1992). Value of e=0.65, which seems a reasonable value for coefficient of restitution is chosen for this study. Finally, the stiffness matrix of the pounding forces $\boldsymbol{K_p}$ is determined in a similar way to the $\boldsymbol{C_p}$ except that c_{sgi} is replaced by k_{sgi}. The vector of separation gap between the adjacent buildings ($\boldsymbol{U_{sg}}$) is

$$\boldsymbol{U_{sg}^T} = \{0 \quad 0 \quad u_{sg1} \quad \cdots \quad u_{sgm} \quad 0 \quad \cdots \quad 0\} \tag{10}$$

u_{sgi} is the separation gap between the adjacent buildings at the ith floor.

The pounding matrices ($\boldsymbol{C_p}$ and $\boldsymbol{K_p}$) and vector ($\boldsymbol{U_{sg}}$) that just introduced are for the case when all adjacent floors pound together. It should be noted that all adjacent floors do not necessarily pound together at the same time. Obviously, pounding is more likely to occur at the top floor of the short building and the corresponding floor of the adjacent tall building. The lower floors are subsequently subjected to pounding one by one during the excitation. In any case, the possibility of pounding should be investigated to find out if other pounding combinations might occur. Pounding forces are developed only at the pounded floors, so the pounding matrices and vector must be changed accordingly.

The mass matrix ($\boldsymbol{M_{bsb}}$) includes mass of buildings and soil as well as SSI term, given by

$$\boldsymbol{M_{bsb}} = \begin{bmatrix} \boldsymbol{m_{ls}} & \boldsymbol{m_{lbs}} & \boldsymbol{0} & \boldsymbol{0} \\ \boldsymbol{m_{lsb}} & \boldsymbol{m_{lb}} & \boldsymbol{0} & \boldsymbol{0} \\ \boldsymbol{0} & \boldsymbol{0} & \boldsymbol{m_{rs}} & \boldsymbol{m_{rbs}} \\ \boldsymbol{0} & \boldsymbol{0} & \boldsymbol{m_{rsb}} & \boldsymbol{m_{rb}} \end{bmatrix} \tag{11}$$

where $\boldsymbol{m_{lb}}$ is the mass matrix of the left building

$$\boldsymbol{m_{lb}} = \begin{bmatrix} m_{l1} & 0 & \cdots & 0 & 0 \\ & m_{l2} & \cdots & 0 & 0 \\ & & \ddots & 0 & 0 \\ & SYM. & & m_{l(n-1)} & 0 \\ & & & & m_{ln} \end{bmatrix} \tag{12}$$

and $\boldsymbol{m_{ls}}$ is the mass matrix of the discrete soil model underneath the left building

$$\boldsymbol{m_{ls}} = \begin{bmatrix} m_{l\varphi} + \sum_{i=1}^{n} H_i^2 m_{li} + I_{li} & \sum_{i=1}^{n} H_i \ m_{li} \\ \sum_{i=1}^{n} H_i \ m_{li} & m_{lf} + \sum_{i=1}^{n} m_{li} \end{bmatrix} \tag{13}$$

and $\boldsymbol{m_{lbs}}$ and $\boldsymbol{m_{lsb}}$ are the mass matrices of the SSI between the left building and soil

$$\boldsymbol{m_{lbs}} = m_{lsb}^{T} = \begin{bmatrix} H_1 m_{l1} & \cdots & H_n m_{ln} \\ m_{l1} & \cdots & m_{ln} \end{bmatrix} \tag{14}$$

m_{li} is the mass of *i*th floor of the left building and $m_{l\varphi}$ and m_{lf} are the rocking and horizontal components of the virtual mass of the discrete soil model underneath the left building, respectively. I_{li} is the mass moment of inertia of *i*th floor of the left building.

The stiffness matrix ($\boldsymbol{K_{bsb}}$) includes the stiffness of buildings and soil as well as the SSSI term, given by

$$\boldsymbol{K_{bsb}} = \begin{bmatrix} \boldsymbol{k_{ls}} & \boldsymbol{0} & \boldsymbol{k_{bsb}} & \boldsymbol{0} \\ \boldsymbol{0} & \boldsymbol{k_{lb}} & \boldsymbol{0} & \boldsymbol{0} \\ \boldsymbol{k_{bsb}} & \boldsymbol{0} & \boldsymbol{k_{rs}} & \boldsymbol{0} \\ \boldsymbol{0} & \boldsymbol{0} & \boldsymbol{0} & \boldsymbol{k_{rb}} \end{bmatrix} \tag{15}$$

where $\boldsymbol{k_{lb}}$ is the stiffness matrix of the left building

$$\boldsymbol{k_{lb}} = \begin{bmatrix} k_{l1} + k_{l2} & -k_{l2} & 0 & \cdots & 0 & 0 \\ & k_{l2} + k_{l3} & -k_{l3} & \cdots & 0 & 0 \\ & & k_{l3} + k_{l4} & \cdots & 0 & 0 \\ & & & \ddots & \vdots & \vdots \\ & SYM. & & & k_{l(n-1)} + k_{ln} & -k_{ln} \\ & & & & & k_{ln} \end{bmatrix} \tag{16}$$

and $\boldsymbol{k_{ls}}$ is the stiffness matrix of the discrete soil model underneath the left building

$$\boldsymbol{k_{ls}} = \begin{bmatrix} k_{l\varphi} & 0 \\ 0 & k_{lf} \end{bmatrix} \tag{17}$$

and $\boldsymbol{k_{bsb}}$ is the stiffness matrix of the SSSI between the adjacent buildings through the soil

$$\boldsymbol{k_{bsb}} = \begin{bmatrix} k_{bsb\varphi} & 0 \\ 0 & k_{bsbf} \end{bmatrix} \tag{18}$$

k_{li} is the stiffness of *i*th floor of the left building and $k_{l\varphi}$ and k_{lf} are the rocking and horizontal components of the stiffness coefficient of the discrete soil model underneath the left building, respectively. $k_{bsb\varphi}$ and k_{bsbf} are the rocking and horizontal components of the stiffness coefficient of the SSSI term, respectively.

The damping matrix ($\boldsymbol{C_{bsb}}$) includes the damping of buildings and soil as well as the SSSI term, given by

$$\boldsymbol{C_{bsb}} = \begin{bmatrix} \boldsymbol{c_{ls}} & \boldsymbol{0} & \boldsymbol{c_{bsb}} & \boldsymbol{0} \\ \boldsymbol{0} & \boldsymbol{c_{lb}} & \boldsymbol{0} & \boldsymbol{0} \\ \boldsymbol{c_{bsb}} & \boldsymbol{0} & \boldsymbol{c_{rs}} & \boldsymbol{0} \\ \boldsymbol{0} & \boldsymbol{0} & \boldsymbol{0} & \boldsymbol{c_{rb}} \end{bmatrix} \tag{19}$$

where $\boldsymbol{c_{lb}}$ is the Rayleigh damping matrix of the left building which is proportional to its mass and stiffness matrices

$$\boldsymbol{c}_{lb} = \alpha_{l0}\boldsymbol{m}_{lb} + \alpha_{l1}\boldsymbol{k}_{lb} \tag{20}$$

and $\boldsymbol{c_{ls}}$ is the damping matrix of the discrete soil model underneath the left building

$$\boldsymbol{c_{ls}} = \begin{bmatrix} c_{l\varphi} & 0 \\ 0 & c_{lf} \end{bmatrix} \tag{21}$$

and $\boldsymbol{c_{bcb}}$ is the damping matrix of the SSSI between the adjacent buildings through the soil

$$\boldsymbol{c_{bsb}} = \begin{bmatrix} c_{bsb\varphi} & 0 \\ 0 & c_{bsbf} \end{bmatrix} \tag{22}$$

α_{l0} and α_{l1} are the Rayleigh coefficients of the left building which are determined from its damping ratio and first two modal circular frequencies . $c_{l\varphi}$ and c_{lf} are the rocking and horizontal components of the damping coefficient of the discrete soil model underneath the left building, respectively. $c_{bsb\varphi}$ and c_{bsbf} are the rocking and horizontal components of the damping coefficient of the SSSI term, respectively.

The coefficients of the discrete soil model ($m_{l\varphi}$, m_{lf} , $k_{l\varphi}$, k_{lf} , $k_{bsb\varphi}$, k_{bsbf} , $c_{l\varphi}$, c_{lf} , $c_{bsb\varphi}$ and c_{bsbf}) can be obtained in time domain by basic constants of soil including its shear modulus (G), shear wave velocity (V_s) and Poisson's ratio (v) and the width of foundation (a) (Naserkhaki and Pourmohammad 2012, Mulliken and Karabalis 1998).

The acceleration, velocity and displacement vectors ($\ddot{\boldsymbol{U}}_{\boldsymbol{bsb}}$, $\dot{\boldsymbol{U}}_{\boldsymbol{bsb}}$ and $\boldsymbol{U}_{\boldsymbol{bsb}}$) of the buildings are as

$$\ddot{\boldsymbol{U}}_{\boldsymbol{bsb}}^{\boldsymbol{T}} = \{\ddot{\boldsymbol{u}}_{\boldsymbol{ls}} \quad \ddot{\boldsymbol{u}}_{\boldsymbol{lb}} \quad \ddot{\boldsymbol{u}}_{\boldsymbol{rs}} \quad \ddot{\boldsymbol{u}}_{\boldsymbol{rb}}\} \tag{23}$$

$$\dot{\boldsymbol{U}}_{\boldsymbol{bsb}}^{\boldsymbol{T}} = \{\dot{\boldsymbol{u}}_{\boldsymbol{ls}} \quad \dot{\boldsymbol{u}}_{\boldsymbol{lb}} \quad \dot{\boldsymbol{u}}_{\boldsymbol{rs}} \quad \dot{\boldsymbol{u}}_{\boldsymbol{rb}}\} \tag{24}$$

$$\boldsymbol{U}_{\boldsymbol{bsb}}^{\boldsymbol{T}} = \{\boldsymbol{u}_{\boldsymbol{ls}} \quad \boldsymbol{u}_{\boldsymbol{lb}} \quad \boldsymbol{u}_{\boldsymbol{rs}} \quad \boldsymbol{u}_{\boldsymbol{rb}}\} \tag{25}$$

where $\ddot{\boldsymbol{u}}_{\boldsymbol{lb}}$, $\dot{\boldsymbol{u}}_{\boldsymbol{lb}}$ and $\boldsymbol{u}_{\boldsymbol{lb}}$ are the acceleration, velocity and displacement vectors of the left building

$$\ddot{\boldsymbol{u}}_{\boldsymbol{lb}}^{\boldsymbol{T}} = \{\ddot{u}_{l1} \quad \cdots \quad \ddot{u}_{ln}\} \tag{26}$$

$$\dot{\boldsymbol{u}}_{\boldsymbol{lb}}^{\boldsymbol{T}} = \{\dot{u}_{l1} \quad \cdots \quad \dot{u}_{ln}\} \tag{27}$$

$$\boldsymbol{u}_{\boldsymbol{lb}}^{\boldsymbol{T}} = \{u_{l1} \quad \cdots \quad u_{ln}\} \tag{28}$$

and $\ddot{\boldsymbol{u}}_{\boldsymbol{ls}}$, $\dot{\boldsymbol{u}}_{\boldsymbol{ls}}$ and $\boldsymbol{u}_{\boldsymbol{ls}}$ are the acceleration, velocity and displacement vectors of the discrete soil model underneath the left building

$$\ddot{\boldsymbol{u}}_{\boldsymbol{ls}}^{\boldsymbol{T}} = \{\ddot{u}_{l\varphi} \quad \ddot{u}_{lf}\} \tag{29}$$

$$\dot{\boldsymbol{u}}_{\boldsymbol{ls}}^{\boldsymbol{T}} = \{\dot{u}_{l\varphi} \quad \dot{u}_{lf}\} \tag{30}$$

$$\boldsymbol{u}_{\boldsymbol{ls}}^{\boldsymbol{T}} = \{u_{l\varphi} \quad u_{lf}\} \tag{31}$$

$\ddot{u}_{li}$, $\dot{u}_{li}$ and u_{li} are the acceleration, velocity and displacement of ith floor of the left building, respectively. $\ddot{u}_{l\varphi}$, $\dot{u}_{l\varphi}$ and $u_{l\varphi}$ are the acceleration, velocity and displacement of the rocking

component of the discrete soil model, respectively, and $\ddot{u}_{lf}$, $\dot{u}_{lf}$ and u_{lf} are the acceleration, velocity and displacement of the horizontal component of the discrete soil model, respectively.

The influence vectors ($\boldsymbol{v_{bsb}}$ and $\boldsymbol{v_{fbsb}}$) of the buildings and soil are as

$$\boldsymbol{v_{bsb}^T} = \{\mathbf{0} \quad \boldsymbol{v_{lb}} \quad \mathbf{0} \quad \boldsymbol{v_{rb}}\} \tag{32}$$

$$\boldsymbol{v_{fbsb}^T} = \{\boldsymbol{v_{ls}} \quad \mathbf{0} \quad \boldsymbol{v_{rs}} \quad \mathbf{0}\} \tag{33}$$

where $\boldsymbol{v_{lb}}$ and $\boldsymbol{v_{ls}}$ are the influence vectors of the left building and soil, respectively

$$\boldsymbol{v_{lb}^T} = \{1 \quad \cdots \quad 1\} \tag{34}$$

$$\boldsymbol{v_{ls}^T} = \{0 \quad m_{lf}\} \tag{35}$$

Finally, the matrices and vectors for the right building ($\boldsymbol{m_{rb}}$, $\boldsymbol{m_{rs}}$, $\boldsymbol{m_{rsb}}$, $\boldsymbol{m_{rbs}}$, $\boldsymbol{c_{rb}}$, $\boldsymbol{c_{rs}}$, $\boldsymbol{k_{rb}}$, $\boldsymbol{k_{rs}}$, $\ddot{\boldsymbol{u}}_{\boldsymbol{rb}}$, $\dot{\boldsymbol{u}}_{\boldsymbol{rb}}$, $\boldsymbol{u_{rb}}$, $\ddot{\boldsymbol{u}}_{\boldsymbol{rs}}$, $\dot{\boldsymbol{u}}_{\boldsymbol{rs}}$, $\boldsymbol{u_{rs}}$, $\boldsymbol{v_{rb}}$, and $\boldsymbol{v_{rs}}$) are determined as same as those determined for the left building except that subscripts *l* (left) and *n* (*n*DOF) are replaced by *r* (right) and *m* (*m*DOF), respectively ($n>m$). Therefore, equation of motion of two adjacent buildings coupled through the soil during earthquake induced pounding (Eq. (3)) is provided with all terms and parameters that are defined and determined.

2.2 Solution of the equation

Seismic responses of the adjacent buildings can be obtained for four cases: i. N-FB, two adjacent buildings with fixed-based (FB) condition which are vibrating individually and freely (no-pounding condition), ii. N-SSSI, two adjacent buildings with SSSI condition which are vibrating individually and freely (no-pounding condition), iii. P-FB, two adjacent buildings with fixed-based (FB) condition which pound together (pounding condition), and iv. P-SSSI, two adjacent buildings with SSSI condition which pound together (pounding condition). The seismic responses of adjacent buildings can be calculated directly from Eq. (3) for the SSSI condition while for the FB condition the matrices and vectors corresponding to the discrete soil model (i.e., those including the subscript *s*) are eliminated. While the adjacent buildings are vibrating individually and freely (no-pounding condition) all terms and components of the pounding matrices ($\boldsymbol{C_p}$ and $\boldsymbol{K_p}$) and vector ($\boldsymbol{U_{sg}}$) are equal to zero. Immediately upon the pounding between the adjacent floors (pounding condition), the pounding forces are developed at the pounded adjacent floors, so the pounding matrices and vector take their values. Arrangement of these values in the pounding matrices and vector depends on the number of pounded adjacent floors and their position. Therefore, occurrence of pounding between each pair of adjacent floors must be checked continuously during the earthquake excitation according to the following condition:

no-pounding condition $$\left(u_{lf} + H_i u_{l\varphi} + u_{li}\right) - \left(u_{rf} + H_i u_{r\varphi} + u_{ri} + u_{sgi}\right) < 0 \tag{36a}$$

pounding condition $$\left(u_{lf} + H_i u_{l\varphi} + u_{li}\right) - \left(u_{rf} + H_i u_{r\varphi} + u_{ri} + u_{sgi}\right) \geq 0 \tag{36b}$$

The pounding matrices and vector take their values based on the number and position of the adjacent floors that are satisfying pounding condition (Eq. (36b)), so they are changed during the earthquake excitation.

Finally, the equation of motion of two adjacent buildings coupled through the soil during

earthquake induced pounding (Eq. (3)) must be solved numerically to obtain seismic responses for the buildings during earthquake excitations. Not only, characteristics of this equation are changed from the no-pounding to the pounding condition and vice versa but also its characteristics are changed during the pounding condition depending on the number and position of the pounded adjacent floors. Thus, the time integration method of Newmark (1959) with linear acceleration of the response at each time step is been used to approximate the solution. Two time steps of 0.01 sec and 0.001 sec are chosen for the no-pounding condition and pounding condition, respectively. These time steps provide accurate results, computational efficiency with minimum calculation time and optimum storage capacity of the output results.

3. Numerical study

Different configurations of the adjacent buildings are considered here, and the seismic responses of the buildings in each configuration are evaluated and discussed. Each configuration comprises two adjacent buildings: the left building, which is always the taller building and the right building, which is the shorter building. The tall building is either 14 or 9 stories high, while the short building has varying stories for different configurations. If the tall building has 14 stories, the number of stories in the short building varies from 2 to 13 stories, and if the tall building has 9 stories, the number of stories in the short building varies from 2 to 8 stories. All of the buildings are assumed to be residential buildings with a mass of 100 tons in each floor, which gives the fundamental periods listed in Table 1. The fundamental periods of the buildings are shown in Table 1 for two conditions, FB and SSSI. Obviously, the fundamental periods of the buildings are longer in the SSSI condition than in the FB condition. Period ratios of each building configuration are also presented in Table 1. The period ratio refers to the ratio of the fundamental period of the short building to the fundamental period of the tall building. Building configurations with

Table 1 Fundamental period of the buildings and period ratios

Story No.	FB			SSSI		
	Fundamental Period (sec)	Period Ratio		Fundamental Period (sec)	Period Ratio	
		Story No. of Tall Building			Story No. of Tall Building	
		14	9		14	9
14	1.347	-	-	1.820	-	-
13	1.260	0.94	-	1.674	0.92	-
12	1.173	0.87	-	1.532	0.84	-
11	1.085	0.81	-	1.393	0.77	-
10	0.994	0.74	-	1.255	0.69	-
9	0.904	0.67	-	1.123	0.62	-
8	0.814	0.60	0.90	0.993	0.55	0.88
7	0.722	0.54	0.80	0.867	0.48	0.77
6	0.628	0.47	0.69	0.742	0.41	0.66
5	0.533	0.40	0.59	0.620	0.34	0.55
4	0.436	0.32	0.48	0.502	0.28	0.45
3	0.336	0.25	0.37	0.385	0.21	0.34
2	0.234	0.17	0.26	0.270	0.15	0.24

relatively smaller period ratios (i.e., closer to 0.2) are considered as out-of-phase building configurations while building configuration with relatively greater period ratios (i.e., closer to 0.9) as in-phase building configurations. The soil is assumed a soft soil with shear wave velocity of 140 m/s, a shear modulus of 32.34 MN/m^2 and a Poisson's ratio of 0.35.

The acceleration records from four earthquakes are selected for the analyses: El Centro (IMPVALL/I-ELC180, PGA=0.313 g, 1940), Northridge (NORTHR/NWH090, PGA=0.583 g, 1994), Kobe (KOBE/KAK090, PGA=0.345 g, 1995) and Chi-Chi (CHICHI/CHY041-N, PGA=0.639 g, 1999). Each building configuration is experiencing the excitation for 15 sec from either earthquake. The seismic responses for the configuration involving a 14-story building adjacent to a 7-story building and subjected to the El Centro earthquake are presented and discussed initially in the following. Then, the minimum required separation gap to prevent pounding between the adjacent buildings of varying height under El Centro earthquake is studied. Finally, the seismic responses of different building configurations with varying heights subjected to four selected earthquakes are covered.

3.1 Seismic responses of a 14-story building adjacent to a 7-story building

The seismic responses of the configuration involving a 14-story building adjusted 0.01 m from a 7-story building subjected to the El Centro earthquake are calculated, and the envelopes for the maximum displacements and story shears of the buildings are shown in Figs. 3 and 4, respectively.

Fig. 3(a) shows that the tall building experiences smaller maximum displacements after pounding and that the displacement reduction is justified through all floor levels of the tall building. Although the FB and SSSI conditions demonstrate a similar pattern, larger displacements are obvious in the SSSI condition. Despite reduction of the displacements, the relative displacements are not reduced throughout the tall building. When the adjacent buildings pound together, the floors below the pounding floor of the tall building are prevented from moving further by the short building, while the floors above the pounding floor move freely. This effect causes a sudden jump between the displacements below and above the pounding floor, as shown in Fig. 3(a). While the relative displacements are reduced in the floors below the pounding floor, this sudden jump causes a sharp increment of relative displacement in the floors above the pounding floor, a whiplash-like effect. Because the story shears are produced due to the relative displacements, they are decreased in the floors below the pounding floor and dramatically increased in the floors above the pounding floor, as shown in Fig. 4(a). In the no-pounding case, the story shear is smaller for the SSSI than for the FB condition for the higher floors because they have smaller relative displacements due to the rocking component of the soil. For the lower floors, the rocking component of the soil is less effective and the story shear can be greater for the SSSI than for the FB condition as it is observed in Fig. 4(a). Anyhow, the pounding suppresses the soil effects particularly effects of the rocking component of the soil because the adjacent pounded building prevents the building to experience the rocking rotation. Thus, story shear can be greater in the SSSI than in the FB condition after pounding. Generally, the most critical condition for the tall building is observed at the floor adjacent to the top floor of the short building, where its story shear is sharply amplified due to pounding. The pounding effect is also critical for the higher floors of the tall building where their story shear is amplified due to pounding.

In the short building, both displacements and story shears are decreased on all floors on the pounding side but increased on the no-pounding side. The short building is prevented from moving on the pounding side, but is pushed away on the no-pounding side, which produces not only larger

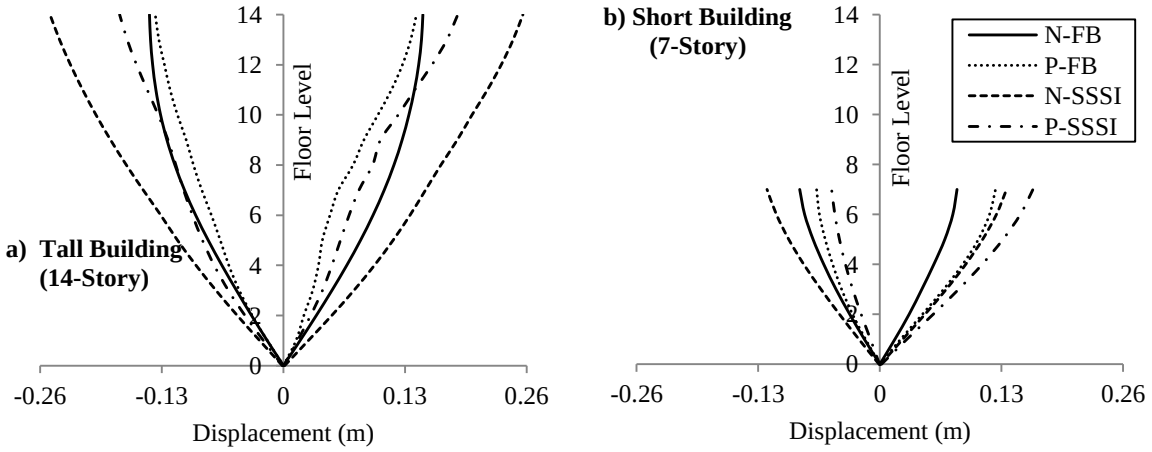

Fig. 3 Envelopes of the maximum displacements of the adjacent buildings

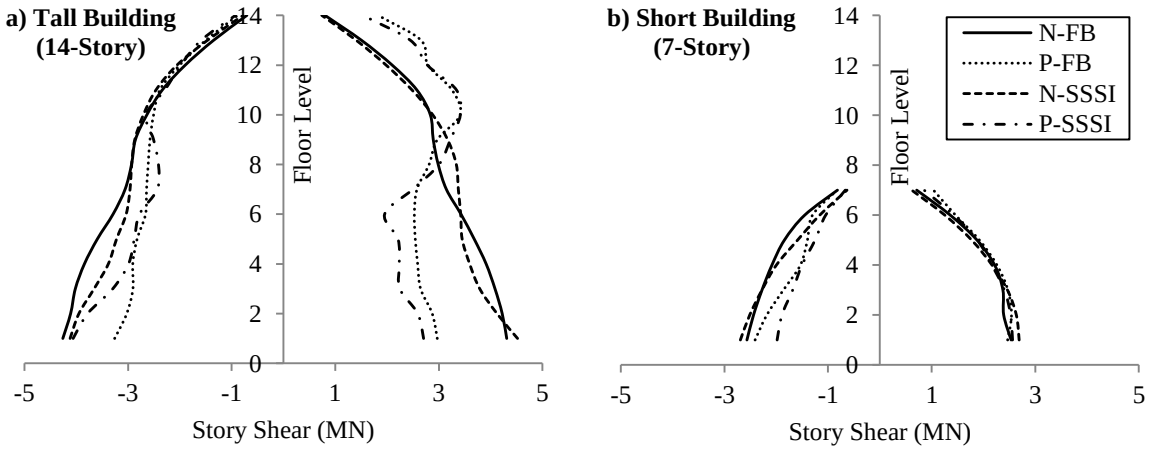

Fig. 4 Envelopes of the maximum story shears of the adjacent buildings

displacements (Fig. 3(b)) but also larger relative displacements, and consequently larger story shears (Fig. 4(b)), on its pounding side. It is also observed that the SSSI condition has larger displacements and story shears than the FB condition on the top floor after pounding. The worst condition occurs at the top floor of the short building, where its displacement and story shear are both amplified due to pounding.

3.2 Minimum required separation gap to prevent pounding between the adjacent buildings of varying height

Separation gap between the adjacent buildings is an important parameter which determines the pounding potential. Actually, the minimum required separation gap to prevent pounding is different for the adjacent buildings of varying height which is studied in this section. The seismic responses of different configurations of adjacent buildings of varying heights (i.e., a 14-story

building or a 9-story building each adjacent to short buildings of varying heights) under El Centro earthquake are calculated to find the minimum required separation gap to prevent pounding. The building configurations involving the 14-story-tall building are referred to as 14-FB and 14-SSSI for the FB and SSSI conditions, respectively. Similarly, the building configurations involving the 9-story-tall building are referred to as 9-FB and 9-SSSI for the FB and SSSI conditions, respectively.

Fig. 5 shows the minimum required separation gap to prevent pounding between the adjacent buildings of varying heights. The minimum required separation gap to prevent pounding is about 0.05±0.01 m for the configurations including the short building with two stories where the buildings are very out of phase. With increment of the number of stories of the short building (from 2 to 6 stories for the short buildings adjacent to 9-story tall building and from 2 to 8 stories for the short buildings adjacent to 14-story tall building) the minimum required separation gap to prevent pounding is increased. For these short buildings with relatively short height the building configurations are still out-of-phase. For the short buildings having 6 or more stories that are adjacent to 9-story tall building and the short buildings having 8 or more stories that are adjacent to 14-story tall building the minimum required separation gap to prevent pounding keeps almost constant with increment of the number of the stories of the short building. This is because the short buildings have relatively tall height so the building configurations are getting in-phase.

It is also found from Fig. 5 that the minimum required separation gap to prevent pounding is dependent to the height of the short building rather than the tall building. No matter if the tall building is a 9 or a 14 story building the minimum required separation gap to prevent pounding is almost the same for a unique short building. The most critical minimum required separation gap to prevent pounding corresponds to the building configurations that have period ratios about 0.55-0.69 (this period ratios refer to the building configurations that height of the short building in these configurations is almost half time the tall building). These findings are in consistence with either existing provisions of minimum required separation gap (SRSS method (International Building Code, IBC 2009), ABS (Taiwan Building Code, TBC 1997) or ratio of building height (Iran National Building Code, INBC 2005). Thus, a similar pattern is expected if any other earthquake excites the buildings. However, in these methods, flexibility of the underneath soil is not included

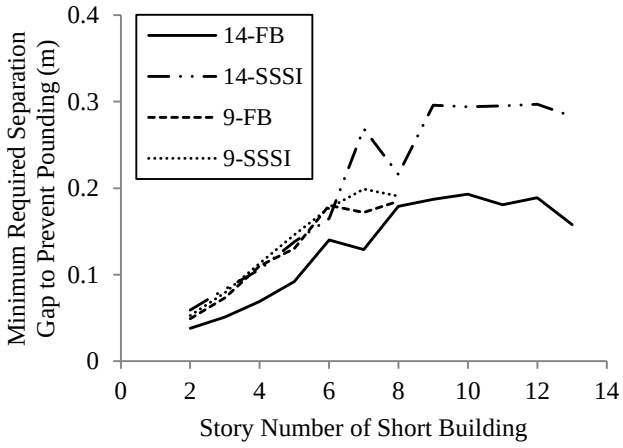

Fig. 5 Minimum required separation gap to prevent pounding between the adjacent buildings of varying heights

(Naserkhaki *et al*. 2013b).

Considering the soil flexibility, it is observed from Fig. 5 that the minimum required separation gap to prevent pounding is wider for the building configuration with the SSSI than the FB condition. When the soil underneath the buildings is very soft (SSSI condition) the phase of the responses are changed and the displacements of the buildings are increased, therefore they are more likely to experience pounding compare to the buildings resting on the hard soil (FB condition). Effect of SSSI condition is more pronounced for the buildings having more stories (taller heights) because their displacements are increased due to rocking component of the soil.

3.3 Seismic responses of adjacent buildings of varying height

The seismic responses of different configurations of adjacent buildings of varying heights are also studied (i.e., a 14-story building and a 9-story building each adjacent to short buildings of varying heights with separation gap of 0.01 m). Each configuration is subjected to the El Centro, Northridge, Kobe and Chi-Chi earthquakes separately. For each configuration, the pounding forces, displacements and story shears are obtained for the four earthquakes. Initially, time histories of the developed pounding forces and displacements are shown and discussed. Then the mean values of the displacement ratios and story shears ratios are presented for different period ratios. The displacement ratio of a building is the ratio of the maximum displacements at the top floor of that building due to a specific earthquake in the pounding case to that of the no-pounding case. The mean value of the displacement ratio provided here is the mean displacement ratio from the four different earthquakes. The story shear ratios are calculated in a similar manner to the displacement ratios. With this normalization (i.e., displacement and story shear ratio) and the assumption that the adjacent buildings behave linear elastic, we are able to compare effect of pounding on their seismic responses due to different earthquakes.

Time histories of the pounding forces represent a good insight to the intensity and duration of the pounding occurrences between the adjacent buildings of varying heights. The pounding forces developed at the top floors of the three different short buildings adjacent to the 14-FB and 14-SSSI buildings during the first 15 sec of the El Centro earthquake are discussed here in order to elaborate on the intensity and duration of the pounding forces in these building configurations. The history of the pounding forces developed at the top floors of the 11-story short buildings is shown in Fig. 6(a). For this building configuration with a period ratio of 0.81, the pounding forces are like impulsive forces with very short durations. The buildings are pounded while separated instantaneously. Pounding forces are less intensive because the buildings vibrate almost in-phase. Although the buildings vibrate relatively in-phase, the initial pounding alters the phase of the response, leading to more poundings during the rest of the earthquake excitation. Alteration of phase of response is shown in Fig. 7(a) where displacement of each building affects the other. Fig. 7(a) clearly shows how the buildings are pounded during the excitation and how the pounding forces are developed in the pounding time. The history of the pounding forces developed at the top floors of the 7-story short buildings is shown in Fig. 6(b). For this building configuration with a period ratio of 0.54, poundings are very intense and have high magnitudes. The duration of each pounding occurrence is longer in this building configuration than in the former building configuration. The history of the pounding forces developed at the top floors of the 4-story short buildings is shown in Fig. 6(c). For this building configuration with a period ratio of 0.32, the poundings are not intense, but they are complete and have long durations. With the buildings are getting out-of-phase, the time when the buildings are in contact with each other is increased. At

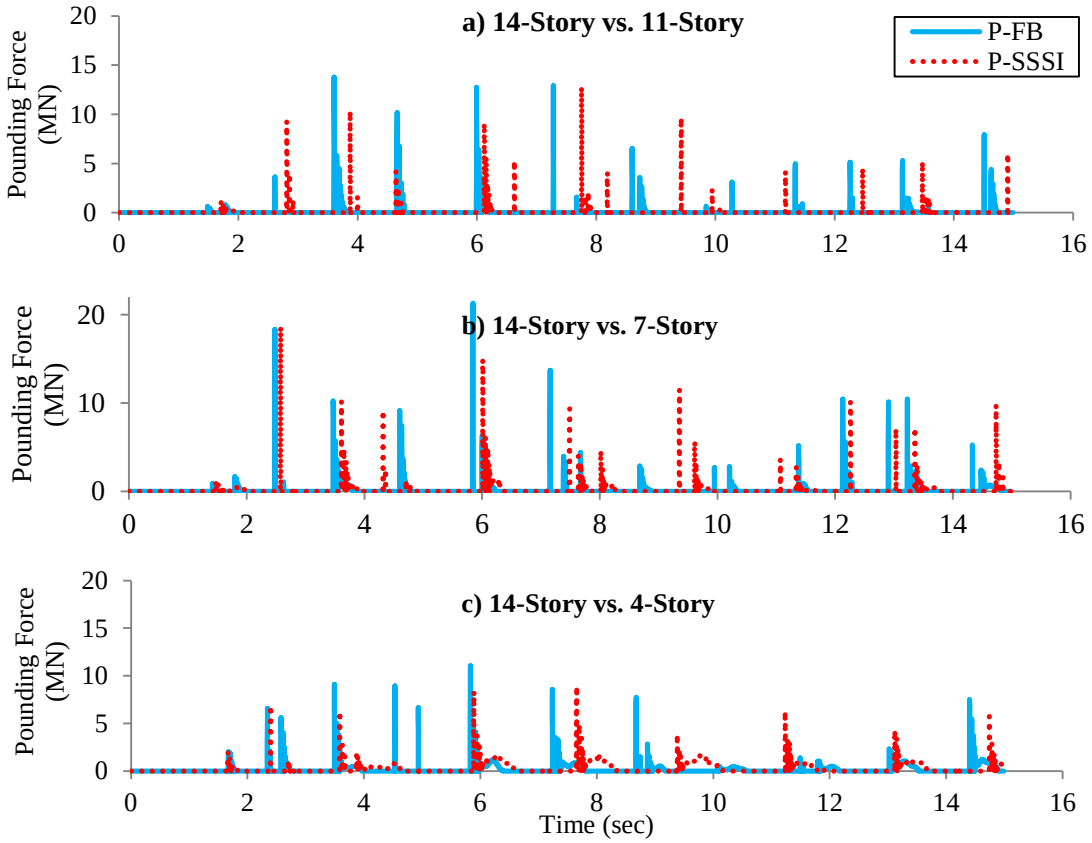

Fig. 6 Time history of the pounding forces developed at the top floor of the short building due to the El Centro Earthquake

low period ratios, small pounding forces develop due to the small total mass of the short building, and the buildings do not separate instantaneously. The peak in pounding force is observed immediately at the beginning of each pounding which is like an impulsive force. After this peak, the buildings are still in contact and pounding force still exists, but its magnitude is now very small.

It is also observed in Fig. 6 that pounding forces developed in the configurations with SSSI effect are less than those developed in configurations with FB effect. This reduction of pounding forces could be explained by relaxation of forces due to soft soil beneath the buildings. Additionally, the time when each pounding occurs and the time when the maximum pounding force is developed are different for FB and SSSI conditions because the soil changes phase of the responses. Also, Fig. 7 shows the soil influence on the building responses more clearly. Not only the displacements are increased due to the soil presence but also the phase of the responses are changed. From this figure it is observed how the adjacent buildings accompany each other during the excitation.

Figs. 8 and 9 indicate variations in the displacement ratios and story shear ratios, respectively, at the top floors of the buildings with respect to the period ratio. The displacement ratios are less than one, but the story shear ratios are greater than one for the tall building because displacements

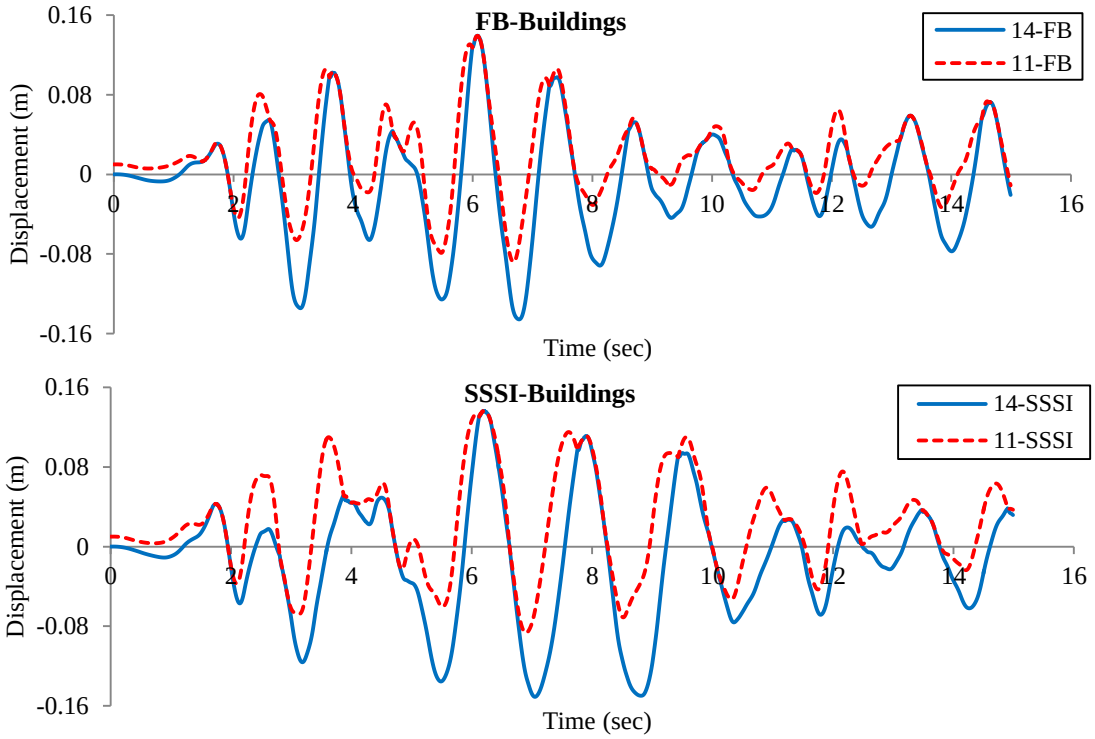

Fig. 7 Time history of the displacement of the buildings at 11th floor (the top floor of the short building) due to the El Centro Earthquake

are reduced and story shears are increased after pounding. Meanwhile, the displacement ratios and story shear ratios are both greater than one for the short building because they are increased after pounding. These trends are similar in both the FB and SSSI conditions; however, the values for the displacement ratios and story shear ratios are more critical in the SSSI condition.

When the adjacent buildings are almost in-phase and the period ratios vary between 0.75 and 0.90, the height of the short building is close to the height of the tall building. Still, the buildings vibrate out-of-phase, and some poundings occur between the adjacent buildings. In this range of the period ratio, weak poundings occur and the effect of pounding is minor in both buildings. The displacements in the tall buildings are smoothly decreased through reduction of the period ratio, with the maximum reduction being 26% for 14-FB and the minimum reduction being 3% for 9-SSSI (Fig. 8(a)). In contrast, the displacements of the short buildings are smoothly increased through reduction of the period ratio, with the maximum increase being 53% for the 11-story short building adjacent to 14-SSSI and the minimum increase being 11% for the 7-story short building adjacent to 9-FB (Fig. 8(b)). Furthermore, the story shears of the tall buildings are rapidly increased by reduction of the period ratio, with the maximum increase being 190% for 14-SSSI and the minimum increase being 55% for 9-FB (Fig. 9(a)). The story shears of the short buildings are smoothly increased by reduction of the period ratio, with the maximum increase being 75% for the 8-story building adjacent to 9-SSSI and the minimum increase being 35% for the 11-story building adjacent to 14-FB (Fig. 9(b)).

The most critical interaction occurs between the adjacent buildings when they become out-of-

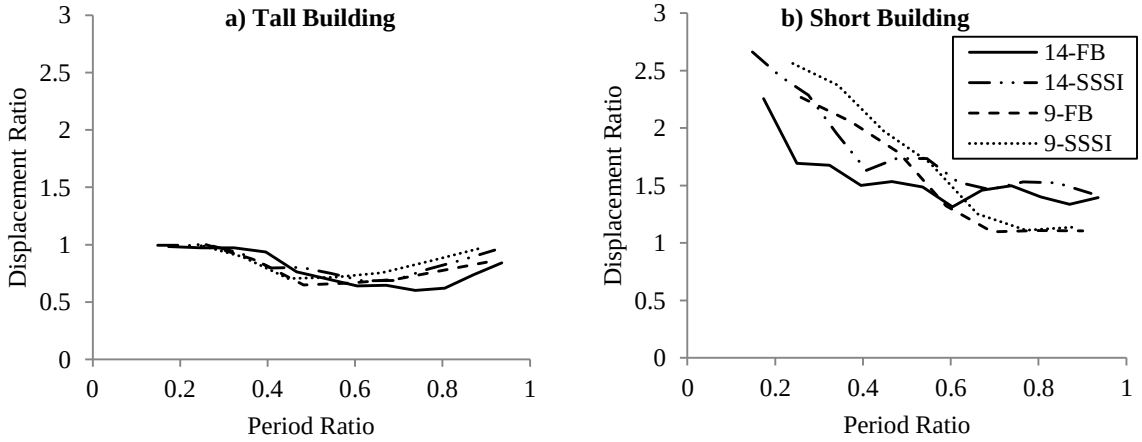

Fig. 8 Relationship between the variation of the displacement ratios in the top floors of the adjacent buildings and the period ratio

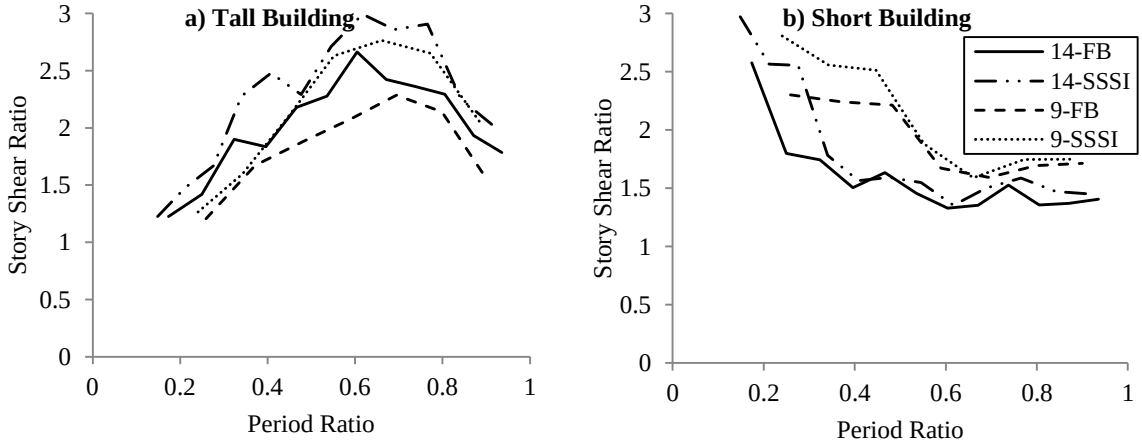

Fig. 9 Relationship between the variation of the story shear ratios in the top floors of the adjacent buildings and the period ratio

phase and the period ratios vary between 0.50 and 0.75. At this range of the period ratio, the height of the short building is approximately one-half the height of the tall building. Both buildings have relatively large masses, and their vibration phases are totally different, resulting in complete and intense poundings between them. The rate of variation in the displacement ratios and story shear ratios is high for both buildings. The tall building suffers the most from pounding at this range of the period ratio in particular. The maximum reduction in displacement and the maximum increase in story shear of the tall building due to pounding are also observed at this range of the period ratio. The maximum reduction of the displacement of the tall building is 40% for 14-FB and the minimum reduction is 25% for 9-SSSI (Fig. 8(a)). The displacements of the short buildings are rapidly increased by reduction of the period ratio, with the maximum increase being 73% for the 8-story short building adjacent to 14-SSSI and the minimum increase being 9% for the 6-story short building adjacent to 9-FB (Fig. 8(b)). Furthermore, the tall buildings experience the highest story

shear due to pounding at this range of the period ratio, with the maximum increase being 199% for 14-SSSI and the minimum increase being 107% for 9-FB (Fig. 9(a)). The story shear of the short building is rapidly increased through reduction of the period ratio, with the maximum increase being 88% for the 5-story building adjacent to 9-SSSI and the minimum increase being 33% for the 8-story building adjacent to 14-FB (Fig. 9(b)).

When the adjacent buildings become too out-of-phase, with period ratios smaller than 0.5, the difference between the height of the tall building and short building becomes substantial. Complete poundings with relatively long durations occur between the buildings. The relatively larger mass of the tall building causes it to govern the movement of both buildings during the pounding. Hence, the tall building is almost unaffected by the pounding, but the short building suffers critically from it. The tall buildings' displacement ratios and story shear ratios approach one during reduction of the period ratio (i.e., the responses of the tall building in the pounding case approach the responses in the no-pounding case), whereas the short buildings' response ratios increase sharply. The maximum reduction of the displacement of the tall building is 24% for 14-FB and the minimum reduction is 0% for all tall buildings regardless of FB or SSSI condition (Fig. 8(a)). The displacements of the short buildings are sharply increased through the reduction of the period ratio, with the maximum increase being 166% for the 2-story short building adjacent to 14-SSSI and the minimum increase being 50% for the 5-story short building adjacent to 14-FB (Fig. 8(b)). Furthermore, the maximum increase of the story shears in the tall buildings due to pounding is 147% for 14-SSSI, and the minimum increment is 20% for 9-FB (Fig. 9(a)). The story shear of the short building is sharply increased through the reduction of the period ratio, with the maximum increase being 197% for the 2-story building adjacent to 14-SSSI and the minimum increase being 50% for the 5-story building adjacent to 14-FB (Fig. 9(b)).

In all the building configurations studied here, it is found that both the tall and short buildings suffer from pounding, and the interaction between the adjacent buildings is most critical when the height of the tall building is almost two times the height of the short building (period ratios about 0.60). The maximum reductions in displacement and the maximum increases in story shear occur in this condition (period ratios about 0.60) for tall buildings. However, the tall buildings are less affected by the pounding and the short buildings are critically and detrimentally affected when the difference between building height is substantial. The shorter the short building, the greater the increase in its displacements and story shears due to pounding. Additionally, the SSSI condition caused more critical changes in the displacements and story shears of both the tall and short buildings than the FB condition. When considering soil effects and coupling, coupling through the soil cause adjacent buildings to experience greater displacements and story shears after pounding.

4. Conclusions

A numerical model of the pounding between adjacent buildings of varying height coupled through the soil is presented in this study. The pounding force is simulated using a linear visco-elastic contact force model that is enabled when the gap between the adjacent buildings is closed. The height of adjacent buildings can vary, causing them to vibrate out-of-phase and pound together. The seismic responses of selected configurations of adjacent buildings with varying heights due to pounding are obtained under four earthquake accelerations.

Although pounding causes the tall building to experience smaller displacements but it causes the building to experience greater story shears at floors above pounding level. The short building

experiences greater displacements and story shears due to pounding. Considering the critical condition at floors where the story shears are increased, the pounding has an unfavorable critical effect on both the tall and short buildings. This is because there is at least one story in almost all studied buildings where the story shear is increased. The SSSI condition causes more critical changes in the buildings than the FB condition. Considering the soil effects and coupling of adjacent buildings through the soil; though reduces the pounding forces, but causes the buildings to experience greater displacements and story shears after pounding.

The minimum required separation gap to prevent pounding depends on the height of the short building. It is increased by increment of height of the short building the building configurations that have period ratios about 0.20 to 0.60. Moreover, wider minimum separation gaps are required for the building configuration with the SSSI than the FB condition.

When the buildings have almost same height, both buildings suffer from pounding while the poundings are of short duration and small magnitude. When the height of the tall building is almost two times the height of the short building (period ratios about 0.60), they pound together intensely while both duration and magnitude of the pounding are increased. The maximum displacement reductions and maximum story shear increments in the tall buildings occur under this condition. When the difference between the heights of the adjacent buildings is substantial, the tall buildings are less affected by the pounding while the short buildings are critically and detrimentally affected. The pounding forces are less intense, but their duration is rather long.

Despite assuming simplified and idealized buildings in this study, results of this research are promising. They confirm the hypothesis that adjacent buildings with different heights are highly susceptible to pounding and the pounding effect is unfavorable for either building. Ignoring pounding effect is very unconservative and could result in terrible consequences.

References

Abdel Raheem, S.E. (2006), "Seismic pounding between adjacent building structures", *Elect. J. Struct. Eng.*, **6**, 66-74.

Anagnostopoulos, S.A. (1988), "Pounding of buildings in series during earthquakes", *Earthq. Eng. Struct. Dyn.*, **16**, 443-456.

Anagnostopoulos, S.A. and Spiliopoulos, K.V. (1992), "An investigation of earthquake induced pounding between adjacent buildings", *Earthq. Eng. Struct. Dyn.*, **21**, 289-302.

Celebi, M., Bazzurro, P., Chiaraluce, L., Clemente, P., Decanini, L., DeSortis, A., Ellsworth, W., Gorini, A., Kalkan, E., Marcucci, S., Milana, G., Mollaioli, F., Olivieri, M., Paolucci, R., Rinaldis, D., Rovelli, A., Sabetta, F. and Stephens, C. (2010), "Recorded motions of the 6 April 2009 Mw 6.3 L'Aquila, Italy, earthquake and implications for building structural damage: overview", *Earthq. Spectra*, **26**(3), 651-684.

Clough, R.W. and Penzien, J. (2003), *Dynamics of Structures*, 3rd Edition, Computers and Structures Inc., California, USA.

Cole, G.L., Dhakal, R.P. and Turner, F.M. (2012), "Building pounding damage observed in the 2011 Christchurch earthquake", *Earthq. Eng. Struct. Dyn.*, **41**, 893-913.

DesRoches, R. and Muthukumar, S. (2002), "Effect of pounding and restrainers on seismic response of multiple-frame bridges", *J. Struct. Eng.*, **128**(7), 860-869.

Favvata, M.J., Karayannis, C.G. and Liolios, A.A. (2009), "Influence of exterior joint effect on the inter-story pounding interaction of structures", *Struct. Eng. Mech.*, **33**(2), 113-136.

Filiatrault, A., Wagner, P. and Cherry, S. (1995), "Analytical prediction of experimental building pounding", *Earthq. Eng. Struct. Dyn.*, **24**, 1131-1154.

IBC (2009), *International Building Code*, International Code Council Inc., Country Club Hills, Illinois,

USA.
INBC (2005), *Loading Chapter: Iranian National Building Code*, Building and Housing Research Center, Tehran, Iran.
Jeng, V. and Tzeng, W.L. (2000), "Assessment of seismic pounding hazard for Taipei city", *Eng. Struct.*, **22**, 459-471.
Jeng, V. and Kasai, K. (1996), "Spectral relative motion of two structures due to seismic travel waves", *J Struct. Eng.*, **122**(10), 1128-1135.
Kasai, K. and Maison, B.F. (1997), "Building pounding damage during the 1989 Loma Prieta earthquake", *Eng. Struct.*, **19**(3), 195-207.
Karayannis, C.G. and Favvata, M.J. (2005a), "Earthquake induced interaction between adjacent reinforced concrete structures with non equal heights", *Earthq. Eng. Struct. Dyn.*, **34**, 1-20.
Karayannis, C.G. and Favvata, M.J. (2005b), "Inter-story pounding between multistory reinforced concrete structures", *Struct. Eng. Mech.*, **20**(5), 505-526.
Komodromos, P., Polycarpou, P.C., Papaloizou, L. and Phocas, M.C. (2007), "Response of seismically isolated buildings considering poundings", *Earthq. Eng. Struct. Dyn.*, **36**:1605-1622.
Maison, B.F. and Kasai, K. (1990), "Analysis for type of structural pounding", *J. Struct. Eng.*, **116**(4), 957-977.
Maison, B.F. and Kasai, K. (1992), "Dynamics of pounding when two buildings collide", *Earthq. Eng. Struct. Dyn.*, **21**, 771-786.
Mirtaheri, S.M., Zandi, A.P., Mavandadi, S., Daryan, A.S. and Ziaei, M. (2012), "Study the possibility of seismic collision between adjacent structures: a case study of Karimkhan avenue in Tehran", *Struct. Design Tall Spec. Build.*, **21**(3), 194-214.
Mix, D., Kijewski-Correa, T. and Taflanidis, A.A. (2011), "Assessment of residential housing in Léogâne, Haiti, and identification of needs for rebuilding after the January 2010 earthquake", *Earthq. Spectra*, **27**(S1), 299-322.
Mouzakis, H.P. and Papadrakakis, M. (2004), "Three dimensional nonlinear building pounding with friction during earthquakes", *J. Earthq. Eng.*, **8**(1), 107-132.
Mulliken, J.S. and Karabalis, D.L. (1998), "Discrete model for dynamic through-the-soil coupling of 3D foundations and structures", *Earthq. Eng. Struct. Dyn.*, **27**, 687-710.
Muthukumar, S. and DesRoches, R. (2006), "A hertz contact model with non-linear damping for pounding simulation", *Earthq. Eng. Struct. Dyn.*, **35**, 811-828.
Naserkhaki, S., Abdul Aziz, F.N. and Pourmohammad, H. (2012a), "Earthquake induced pounding between adjacent buildings considering soil structure interaction", *Earthq. Eng. Eng. Vib.*, **11**(3), 343-358.
Naserkhaki, S., Abdul Aziz, F.N. and Pourmohammad, H. (2012b), "Parametric study on earthquake induced pounding between adjacent buildings", *Struct. Eng. Mech.*, **43**(4), 503-526.
Naserkhaki, S., Daneshvar-Ghorbani, S. and Tayyebi-Tolloei, D. (2013a), "Heavier adjacent building pounding due to earthquake excitation", *Asian J. Civil Eng.* (BHRC), **14**(2), 349-367.
Naserkhaki, S., El-Rich, M., Abdul Aziz, F.N. and Pourmohammad, H. (2013b), "Separation gap, a critical factor in earthquake induced pounding between adjacent buildings", *Asian J. Civil Eng.* (BHRC), **14**(6), 881-898.
Naserkhaki, S. and Pourmohammad, H. (2012), "SSI and SSSI effects in seismic analysis of twin buildings: discrete model concept", *J. Civil Eng. Manag.*, **18**(6), 890-898.
Newmark, N.M. (1959), "A method of computation for structural dynamics", *J. Eng. Mech.*, **85**, 67-94.
Nguyen, D.T., Noah, S.T. and Kettleborough, C.F. (1986), "Impact behaviour of an oscillator with limiting stops, Part I: a parametric study", *J. Sound Vib.*, **109**(2), 293-307.
Padron, L.A., Aznarez, J.J. and Maeso, O. (2009), "Dynamic structure soil structure interaction between nearby piled buildings under seismic excitation by BEM-FEM model", *Soil Dyn. Earthq. Eng.*, **29**, 1084-1096.
Polycarpou, P.C. and Komodromos, P. (2010), "Earthquake induced poundings of a seismically isolated building with adjacent structures", *Eng. Struct.*, **32**, 1937-1951.
Rahman, A.M., Carr, A.J. and Moss, P.J. (2001), "Seismic pounding of a case of adjacent multiple-story

building of differing total heights considering soil flexibility effects", *Bull. New Zealand Soc. Earthq. Eng.*, **34**(1), 40-59.
Rajalingham, C. and Rakheja, S. (2000), "Analysis of impact force variation during collision of two bodies using a single degree of freedom system model", *J. Sound Vib.*, **229**(4), 823-835.
Rosenblueth, E. and Meli, R. (1986), "The 1985 earthquake: causes and effects in Mexico City", *Concrete Int.*, ACI, **8**(5), 23-36.
Ruangrassamee, A. and Kawashima, K. (2003), "Control of nonlinear bridge response with pounding effect by variable dampers", *Eng. Struct.*, **25**, 593-606.
Savin, E. (2003), "Influence of free field variability on linear Soil-Structure Interaction (SSI) by indirect integral representation", *Earthq. Eng. Struct. Dyn.*, **32**, 49-69.
Shakya, K. and Wijeyewickrema, A.C. (2009), "Mid-column pounding of multi-story reinforced concrete buildings considering soil effects", *Adv. Struct. Eng.*, **12**(1), 71-85.
TBC.(1997), Seismic Provisions: Taiwan Building Code, Construction and Planning Administration Ministry of Interior, Taiwan.
Zhao, B., Taucer, F. and Rossetto, T. (2009), "Field investigation on the performance of building structures during the 12 May 2008 Wenchuan earthquake in China", *Eng. Struct.*, **31**, 1707-1723.
Zhu, P., Abe, M. and Fujino, Y. (2002), "Modelling three-dimensional non-linear seismic performance of elevated bridges with emphasis on pounding of girders", *Earthq. Eng. Struct. Dyn.*, **31**, 1891-1913.

CC